Cooper pair sizes in superfluid nuclei in a simplified model

X. Viñas,[1] P. Schuck,[2,3,4] and N. Pillet[5]

[1]*Departament d'Estructura i Constituents de la Matèria and Institut de Ciències del Cosmos, Facultat de Física, Universitat de Barcelona, Diagonal 647, E-08028 Barcelona, Spain*

[2]*Institut de Physique Nucléaire, CNRS, UMR8608, Orsay, F-91406, France*

[3]*Université Paris-Sud, Orsay, F-91505, France*

[4]*Laboratoire de Physique et Modélisation des Milieux Condensés, CNRS and Université Joseph Fourier, Maison des Magistères, Boîte Postale 166, F-38042 Grenoble Cedex, France*

[5]*CEA/DAM/DIF, F-91297 Arpajon, France*

(Received 19 January 2010; revised manuscript received 25 June 2010; published 14 September 2010)

Cooper pair sizes are evaluated in a simple harmonic oscillator model reproducing the values of sophisticated Hartree-Fock-Bogoliubov calculations. Underlying reasons for the very small sizes of 2.0–2.5 fm of Cooper pairs in the surface of nuclei are analyzed. It is shown that the confining properties of the nuclear volume is the dominating effect. It is argued that for Cooper pair sizes the local-density approximation idea is particularly inadapted.

DOI: 10.1103/PhysRevC.82.034314 PACS number(s): 21.30.Fe, 21.10.Re, 21.60.Jz, 24.30.Cz

Recent studies have revealed surprisingly small extensions of Cooper pairs in the surface of superfluid nuclei [1–3]. Such features are potentially very important in pair transfers in nuclear reactions [4]. Though the reason for the small sizes was identified in our preceding paper [5] to be from the finite size of nuclei, it is nevertheless instructive to further elaborate on the underlying reasons for this behavior. We, therefore, develop a simplified model that has all the essential ingredients for the comprehension of the effect. The model consists of a spherical harmonic oscillator (HO) potential (without spin orbit) for the mean field together with a realistic treatment of pairing using the Gogny D1S force [6]. We will see that such a model quite accurately reproduces the results for the so-called coherence length (CL), that is, the size of Cooper pairs, of much more sophisticated self-consistent Hartree-Fock-Bogoliubov (HFB) calculations [1].

The questions we will try to answer are the following:

(i) What is the reason for the existence of such very small-sized Cooper pairs with extensions 2.0–2.5 fm in the surface of nuclei, about a factor 2–3 times smaller than the smallest size in nuclear matter at low densities? Those values are also much smaller than the ones estimated from the common belief that Cooper pair sizes in nuclei are of about the nucleus' dimension [7], what is based on pairing in nuclei being in the weak coupling regime. Because in weak coupling CL $> b$, with b the oscillator length to be used below, the fact that for a nucleus with, for example, nucleon number $A = 120$, $b \sim 2.2$ fm $\sim$CL$_{\min.}$, does it lead to the conclusion that the surface pairing is close to strong coupling? Those small sizes also are of similar magnitude as that of the deuteron, that is, a bound state. Does it mean that the neutron Cooper pairs are locally also eventually in a bound state? Actually, this might not be completely surprising because two neutrons are almost bound even in free space and pairing could help to make them truly bound. The question then is whether the small size of the CLs is from particularly strong pairing in the nuclear surface (local strong coupling) or whether it is essentially from the confining constraints from the nuclear volume? It will be shown that the small sizes are dominantly from the latter effect.

(ii) The minimum of the CL, $\xi(R)$, in local-density approximation (LDA) is about at the same density as the one in the quantal case [5]. Then, is the qualitative resemblance of $\xi(R)$ calculated from nuclear matter in LDA and the quantal $\xi(R)$ a fortuitous coincidence, or is that a manifestation of similar pairing correlations in both cases? We will see that the quantal behavior of $\xi(R)$ in finite nuclei is very similar for nominal and almost vanishing pairing. In the latter case one should not talk about coherence length but simply of the root-mean-square (rms) distance of uncorrelated pairs coupled to angular momentum $L = 0$, which is entirely determined by the single-particle mean-field wave functions.

We begin our considerations with the density matrix corresponding to one major shell of a spherical HO potential $V(R) = \frac{m}{2}\omega^2 R^2$ with $\hbar\omega = 41A^{-1/3}$ MeV,

$$\hat{\rho}_N = \sum_{nlm}{}' |nlm\rangle\langle nlm|, \tag{1}$$

where the prime on the sum indicates that it only runs over all the states $|nlm\rangle$ contained in the major shell N.

We start out transforming this density matrix into Wigner (W) space. W space, or phase space, is useful for certain aspects and furthermore it has a well-known analytic form for the case of an HO potential where it only depends on the classical Hamiltonian $H_{\text{cl.}} = p^2/2m + V(R)$. The corresponding W distribution is given by [8]

$$\hat{\rho}_N|_W = f_N(H_{\text{cl.}}) = 8(-1)^N e^{-\frac{2H_{\text{cl.}}}{\hbar\omega}} L_N^{(2)}\left(\frac{4H_{\text{cl.}}}{\hbar\omega}\right), \tag{2}$$

where $L_n^{(\lambda)}(x)$ are the generalized Laguerre polynomials.

We are now ready to present our simplified pairing model. We shall write the W transform [9] of the anomalous density matrix $\kappa(\mathbf{r},\mathbf{r}') = \langle \mathrm{BCS}|a^+(\mathbf{r})a^+(\mathbf{r}')|\mathrm{BCS}\rangle$ as (spin-singlet wave function is suppressed),

$$\kappa(\mathbf{R},\mathbf{p}) = \sum_N \kappa_N f_N(H_{\mathrm{cl.}}), \tag{3}$$

with $\kappa_N = u_N v_N$ and u_N, v_N the usual BCS amplitudes. Please note that the degeneracy factors are missing in Eq. (3). This stems from the fact that expression (2) is not normalized to unity but to the degeneracy of the shell N.

The gap parameters Δ_N can be obtained from the solution of a gap equation with matrix elements averaged over major shells [10].

$$\Delta_N = \sum_{N'} D_{N'} V_{N,N'} \frac{\Delta_{N'}}{2\sqrt{(E_{N'}-\mu)^2+\Delta_{N'}^2}}, \tag{4}$$

where $E_N = (3/2+N)\hbar\omega$, $D_N = (N+1)(N+2)/2$ is the degeneracy factor of major shell N, and $V_{N,N'}$ is the shell-averaged pairing matrix element. To obtain $V_{N,N}$ we start from the state-dependent pairing matrix element [9],

$$\langle \Phi(\nu,\bar{\nu})|v|\Phi(\nu',\bar{\nu}')\rangle = \langle \nu,\bar{\nu}|v|\nu',\bar{\nu}'\rangle - \langle \nu,\bar{\nu}|v|\bar{\nu}',\nu'\rangle, \tag{5}$$

where the two-particle states $|\nu,\bar{\nu}\rangle$ are product states $|\nu\rangle$ and $|\bar{\nu}\rangle$. The states $|\nu\rangle$ are represented by single-particle wave functions $\phi_\nu(\vec{r},\sigma) = \phi_{nlm}(\vec{r})\psi_\sigma$ and the corresponding time reversal states by $\phi_{\bar{\nu}}(\vec{r}',\sigma) = (-1)^{1/2-\sigma}\phi^*_{nlm}(\vec{r}')\psi_{-\sigma}$. Averaging over the energy shells E_N and E'_N, it is easy to show that in phase space the shell-averaged pairing matrix elements read (see [10] for more details)

$$V_{N,N'} = \frac{1}{D_N D_{N'}} \int d^3R \int \frac{d^3p d^3p'}{(2\pi\hbar)^6} f_N(H_{\mathrm{cl.}}) f_{N'}(H'_{\mathrm{cl.}}) \times v_\eta(\mathbf{p}-\mathbf{p}'), \tag{6}$$

with $v_\eta(p) = \eta v(p)$ and $v(p)$ being the Fourier transform of the Gogny D1S interaction in the $^1S_0$ pairing channel [6]. The factor η serves to adjust the pairing intensity by hand.

In Fig. 1, we give the gap at the Fermi energy Δ_F as a function of A. We take $\eta = 0.85$ to compensate for the fact that we use the bare mass, $m^* = m$ what usually overestimates pairing. We see that the typical arch structure is recovered. Without any averaging, the gap values would depend on the individual single-particle quantum numbers n, l and Fig. 1 would show an additional fine structure. In the present case an averaging over the individual substates of one major shell was performed not wiping out, however, the essential quantum features.

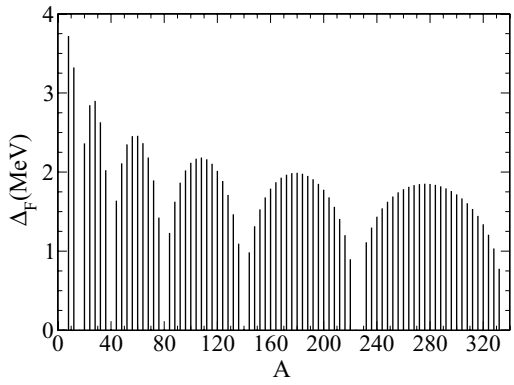

FIG. 1. Pairing gap at the Fermi energy computed using the Gogny D1S force as a function of the number of nucleons A in an isotropic HO potential.

We now proceed to the calculation of the CL. Interpreting the anomalous density as the wave function of a Cooper pair (we are aware of the fact that this point of view was debated recently [11]), the local rms value of a pair is given by [1]

$$\xi(R) \equiv \sqrt{\frac{N(R)}{D(R)}} = \sqrt{\frac{\int d^3s\, s^2\kappa^2(\mathbf{R},\mathbf{s})}{\int d^3s\,\kappa^2(\mathbf{R},\mathbf{s})}} = \sqrt{\frac{\int \frac{d^3p}{(2\pi\hbar)^3}|d\kappa(H_{\mathrm{cl.}})/d(p/\hbar)|^2}{\int \frac{d^3p}{(2\pi\hbar)^3}\kappa^2(H_{\mathrm{cl.}})}}. \tag{7}$$

Here, $2\mathbf{R} = \mathbf{r}+\mathbf{r}'$ and $\mathbf{s} = \mathbf{r}-\mathbf{r}'$ and $\kappa(\mathbf{R},\mathbf{s})$ is the Fourier transform of $\kappa(\mathbf{R},\mathbf{p})$ of (3).

Using Eqs. (2) and (3), denominator and numerator under the square root in Eq. (7) can be obtained explicitly in the case of the HO potential:

$$D(R) = \frac{4\alpha^3}{\pi^2}\sqrt{\frac{\pi}{2}}e^{-2\alpha^2R^2}\sum_K\sum_J(-1)^{K+J}\kappa_K\kappa_J \times \sum_{K1=0}^{\min(K,J)} L^{(1/2)}_{K1}(0)L^{(1/2)}_{K-K1}(2\alpha^2R^2)L^{(1/2)}_{J-K1}(2\alpha^2R^2), \tag{8}$$

$$N(R) = \frac{12\alpha}{\pi^2}\sqrt{\frac{\pi}{2}}e^{-2\alpha^2R^2}\sum_K\sum_J(-1)^{K+J}\kappa_K\kappa_J \times \sum_{K1=0}^{\min(K,J)} L^{(3/2)}_{K1}(0)\big[L^{(1/2)}_{K-K1}(2\alpha^2R^2) + L^{(1/2)}_{K-K1-1}(2\alpha^2R^2)\big]\big[L^{(1/2)}_{J-K1}(2\alpha^2R^2) + L^{(1/2)}_{J-K1-1}(2\alpha^2R^2)\big], \tag{9}$$

where $\alpha = 1/b = \sqrt{m\omega/\hbar}$ is the inverse HO length, K and J are the principal HO quantum numbers of the shells, κ_K and κ_J the corresponding BCS amplitudes of the pairing tensor.

In the top panel of Fig. 2 we show $\xi(R)$ for different values of η. It is seen that $\xi(R)$ only depends very weakly on the pairing strength for $\eta < 1$, this happens for instance around the minimum and the similarity with the results of the realistic calculations presented in [1] and displayed again in the bottom panel of Fig. 2, is striking. In particular, our model reproduces the very small value of $\xi(R)$ in the nuclear surface of about 2 fm. For $\eta > 1$, the CL starts to move to lower values in the interior. However, the minimum again only is very little affected.

In our model it is now rather straightforward to understand where this striking *independence* of $\xi(R)$ on the intensity of pairing comes from. From Eq. (2), we can realize that the features of $f_{N_F}(H_{\mathrm{cl.}})$, where N_F corresponds to the major shell

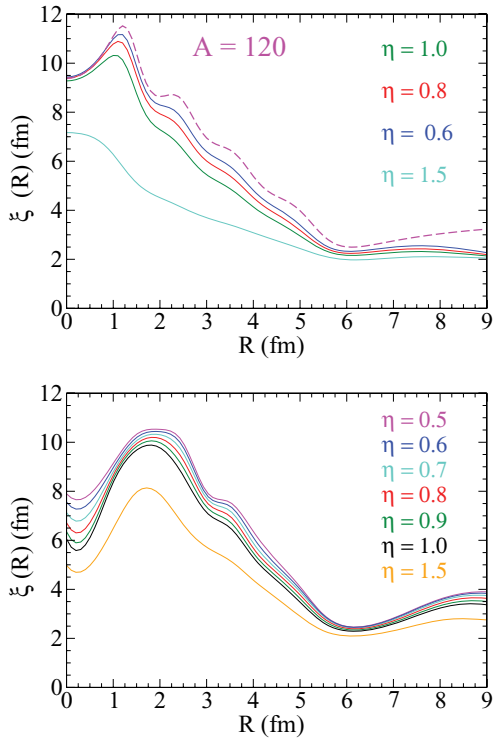

FIG. 2. (Color online) Coherence length for different strengths of the pairing force as a function of the radial distance R for a symmetric nucleus with $A = 120$. The dashed line corresponds to the no-pairing limit (top). HFB coherence length for the nucleus ^{120}Sn computed for several strengths of the pairing D1S Gogny force (bottom).

at the Fermi energy, have a width of order $\sim \hbar\omega$ (one may check this explicitly for some low-order $L_N^{(2)}$ polynomials). Because in the case of nuclei $\Delta_N \ll \hbar\omega$, the κ_N are essentially only active at the Fermi level and we approximately have from Eq. (3) that $\kappa(\mathbf{R}, \mathbf{p})$ is proportional to $f_{N_F}(H_{\text{cl.}})$. In the limit $\eta \to 0$, we have the equality (strictly speaking one should in this limit change the name and not call it coherence length because there is no coherence any longer; however, for convenience, we will not change the letter ξ nor the name):

$$\begin{aligned}\xi(R) &\overset{\lim_{\eta\to 0}}{=} \sqrt{\frac{\int \frac{d^3p}{(2\pi\hbar)^3}\left[df_{N_F}(H_{\text{cl.}})/d(p/\hbar)\right]^2}{\int \frac{d^3p}{(2\pi\hbar)^3}\left[f_{N_F}(H_{\text{cl.}})\right]^2}} \\ &= \frac{\hbar^2}{m}\sqrt{\frac{\int_{V(R)}^{\infty} dH_{\text{cl.}} k^3_{H_{\text{cl.}}}(R)\left[df_{N_F}(H_{\text{cl.}})/dH_{\text{cl.}}\right]^2}{\int_{V(R)}^{\infty} dH_{\text{cl.}} k_{H_{\text{cl.}}}(R)\left[f_{N_F}(H_{\text{cl.}})\right]^2}} \\ &= \sqrt{\frac{\int d^3s s^2 \left|\rho_{N_F}(\mathbf{R}, \mathbf{s})\right|^2}{\int d^3s \left|\rho_{N_F}(\mathbf{R}, \mathbf{s})\right|^2}}, \end{aligned} \tag{10}$$

where $k_{H_{\text{cl.}}}(R) = \sqrt{\frac{2m}{\hbar^2}[H_{\text{cl.}} - V(R)]}$ and $\rho_{N_F}(\mathbf{R}, \mathbf{s})$ is the Fourier transform of $f_{N_F}(H_{\text{cl.}})$ with respect to momentum p, that is, the density matrix corresponding to the Fermi level $N = N_F$. The latter can be obtained from Eq. (2) as

$$\begin{aligned}\rho_N(\mathbf{R}, \mathbf{s}) = \frac{\alpha^3}{\pi^{3/2}} e^{-(R^2 + \frac{s^2}{4})} \sum_{K_1=0}^{K_1=N} (-1)^{N-K_1} \\ \times L^{1/2}_{N-K_1}(2\alpha^2 R^2) L^{1/2}_{K_1}\left(\frac{\alpha^2 s^2}{2}\right). \end{aligned} \tag{11}$$

With a rescaling of the relative coordinate $s \to 2s$, we see the well-known fact (see, e.g., [5]) that the density matrix for even/odd N is completely symmetric/antisymmetric with respect to an interchange of relative and center-of-mass (c.m.) coordinates s and R. From Eq. (10) it can be seen that the dependence of $\xi(R)$ on Δ has dropped out completely. This stems from the fact that in our HO model with its degenerate shells, in the limit $\eta \to 0$, the chemical potential becomes locked exactly at the Fermi level (i.e., at the shell N_F). In general, this is not the case in a Woods-Saxon potential where it can happen that the chemical potential becomes situated in between two subshells. In the top panel of Fig. 2, we also show the limiting value of the coherence length (dashed line) when $\Delta \to 0$. It is clear that this asymptotic form of the CL is very close to the other curves, in particular, at the minimum. Therefore, in nuclear physics, in what concerns the CL, we are always almost in the asymptotic limit of vanishing pairing. In a sense, the closeness of the CL to the corresponding uncorrelated value is one of the most striking manifestations that nuclei are in the weak coupling regime of pairing. Of course, this should not make us forget that on other quantities nuclear pairing has a strong influence. A particularly pertinent example, discussed recently [3,5], is the strong influence of parity mixing on the spatial features of the (*non-normalized*) pairing tensor.

Let us now try to analyze from where comes this typical behavior of the CL [i.e., of $\xi(R)$]. It rises from $R = 0$ up to $R = 1-2$ fm, followed by a longer almost linear descent, passing through a shallow minimum of 2–2.5 fm, leveling off at some slightly higher asymptotic value. Before coming to this study, let us mention again that this behavior seems to be very robust being found in realistic HFB calculations in nuclei (see Fig. 3 in [1]) in a slab geometry [12], as well as in the present very simplified HO model.

Let us consider the normalized square of the density matrix, as it enters the definition of the CL. From Eqs. (10) and (11) we obtain

$$\begin{aligned}&\frac{|\rho_N(\mathbf{R}, \mathbf{s})|^2}{\int d^3s |\rho_N(\mathbf{R}, \mathbf{s})|^2} \\ &= \frac{\alpha^3}{4\pi}\sqrt{\frac{2}{\pi}} e^{-\frac{\alpha^2 s^2}{2}} \\ &\times \frac{\left(\sum_{K_1=0}^{K_1=N} (-1)^{N-K_1} L^{(1/2)}_{N-K_1}(2\alpha^2 R^2) L^{(1/2)}_{K_1}\left(\frac{\alpha^2 s^2}{2}\right)\right)^2}{\sum_{K_1=0}^{K_1=N}\left(L^{(1/2)}_{N-K_1}(2\alpha^2 R^2)\right)^2 L^{(1/2)}_{K_1}(0)}. \end{aligned} \tag{12}$$

In the particularly simple case of $N = 1$, $L_1^{(1/2)}(x) = \frac{3}{2} - x$ and $L_0^{(1/2)}(x) = 1$, and consequently Eq. (12), after multiplying

by s^4, reads

$$\frac{|\rho_1(\mathbf{R},\mathbf{s})|^2 s^4}{\int ds |\rho_1(\mathbf{R},\mathbf{s})|^2 s^2} = \alpha^3 \sqrt{\frac{2}{\pi}} e^{-\frac{\alpha^2 s^2}{2}} \frac{\alpha^4 (2R^2 - s^2/2)^2 s^4}{4\alpha^4 R^4 - 6\alpha^2 R^2 + 3.75}. \tag{13}$$

One sees that Eq. (12) has an R-dependent node at $s = 2R$, a feature that is important for interpreting the characteristic behavior of the CL. After integrating Eq. (12) over s, one obtains for the CL,

$$\begin{aligned} \xi^2(R) &= \frac{\int ds (2R^2 - s^2/2)^2 s^4 e^{-\alpha^2 s^2/2}}{\int ds (2R^2 - s^2/2) s^2 e^{-\alpha^2 s^2/2}} \\ &= \frac{3}{\alpha^2} \times \frac{4x^2 - 20x + 35}{4x^2 - 12x + 15}, \end{aligned} \tag{14}$$

where $x = 2\alpha^2 R^2$. Minimization with respect to R implies that

$$4x^2 - 20x + 15 = 0, \tag{15}$$

the roots of which are $x_1 = 2.5 - \sqrt{2.5} = 0.9189$ and $x_2 = 2.5 + \sqrt{2.5} = 4.0818$, x_1 corresponding to the maximum and x_2 to the minimum.

In the case of $N = 1$, let us take, somewhat arbitrarily, the symmetric open-shell nucleus $A = 12$ (to fix the value of $\omega \propto A^{-1/3}$). From the definition of x one obtains for the position R and the values of maximum and minimum of the CL,

$$R_{\max} = 1.0315 \text{ fm} \qquad \xi(R)_{\max} = 4.3476 \text{ fm}, \tag{16}$$

and

$$R_{\min} = 2.1740 \text{ fm} \qquad \xi(R)_{\min} = 2.0629 \text{ fm}. \tag{17}$$

The coherence length corresponding to $A = 12$ ($N = 1$) is displayed in Fig. 3. It is very surprising that even for this simplest case of $N = 1$ the essential features of the CL are already born out. For instance, the minimal value is at about 2 fm, as in all other cases, realistic ones included [5]. On the other hand for $N = 0$, no R dependence of the CL exists. The constant value of CL for $N = 0$ is about 2 fm for, for example, $A = 4$ (i.e., the α particle). Therefore, one needs at least to go to P-shell nuclei (i.e., $N = 1$) so that in the interior the pairs can extend beyond 2 fm. However, coming close to the edge of the nucleus, the rms value of the pair gets (approximately) back to its value it has in the α particle.

The coherence length for $A = 28$ that corresponds to a midshell nucleus with $N = 2$ reads

$$\xi^2(R) = \frac{3}{\alpha^2} \frac{16x^4 - 224x^3 + 1160x^2 - 2312x + 2009}{16x^4 - 160x^3 + 616x^2 - 888x + 561}, \tag{18}$$

where again $x = 2\alpha^2 R^2$. The minimization with respect to R implies that

$$\begin{aligned} &64x^6 - 1088x^5 + 7248x^4 - 27168x^3 + 61340x^2 \\ &\quad - 73348x + 30435 = 0, \end{aligned} \tag{19}$$

which yields the only real roots: $x_1 = 0.7822$ and $x_2 = 7.5622$, x_1 corresponding to the maximum and x_2 to the minimum. The other four roots of Eq. (19) are complex.

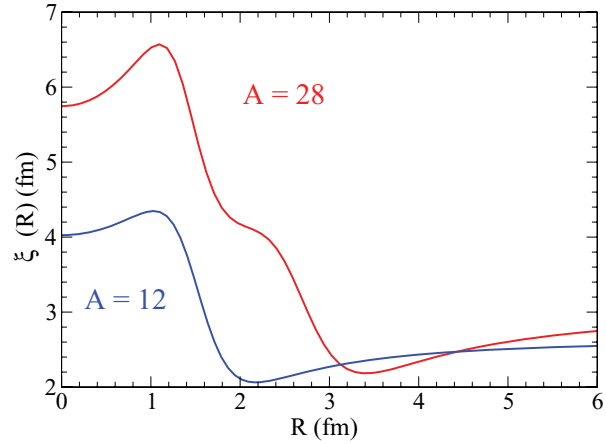

FIG. 3. (Color online) Coherence length (fm) for systems containing $A = 12$ and $A = 28$ nucleons as a function of the distance to the center R (fm).

From the previous definition of x one obtains

$$R_{\max} = 1.0960 \text{ fm}, \qquad \xi(R)_{\max} = 6.5700 \text{ fm}, \tag{20}$$

and

$$R_{\min} = 3.4079 \text{ fm}, \qquad \xi(R)_{\min} = 2.1838 \text{ fm}. \tag{21}$$

The coherence length corresponding to this case is also displayed in Fig. 3. To better understand the qualitatively similar behavior of the CL for the $A = 12$ and $A = 28$ cases, we show in Fig. 4 expression (12) and the corresponding one for $A = 28$ as a function of s for various values of R. The area below the curves in Fig. 4 directly yields the CL. The striking feature is that the scenario is qualitatively much the same in both cases, in spite of the fact that for $N = 2$ there are two nodes instead of one [13]. The analysis shows that the two nodes also move proportional to R from inside to outside in a similar way as for the $N = 1$ case. We surmise that the behavior stays more or less the same also for higher N values. There are two asymptotic regimes where the nodal structure in s practically does not influence the integrand in s [i.e., (12)] and that are more or less dominated by a single bump structure. This is the case for very small R values as well as for large R values, approximately from the minimum point of the CL onwards. In between, the behavior switches from one regime to the other. This is where the CL shrinks about linearly with R. To exhibit the linear behavior more clearly, we show in Fig. 5 the CLs for $A = 12$, 28, 120, and 8000. We scale in that figure the CL and the R coordinate by the radius at the classical turning point, $R_t = \sqrt{\frac{2\mu}{m\omega^2}}$, given by the intersection of the chemical potential $\mu = 46.933$ MeV (remember that with an HO potential, μ is independent of the nucleon number A) with the HO potential and, thus, representing the size of the system. It is seen that the different curves almost are superposed averaging around a linear descent. Only the beginning and the ends vary. The position of the minimum ranges between a little more than half of R_t for $A = 12$ to about 90% of R_t for $A = 8000$. In the interior, close to the origin, the pairs occupy the whole nuclear volume; while approaching the surface they steadily shrink to about 2–2.5 fm from the close presence of the

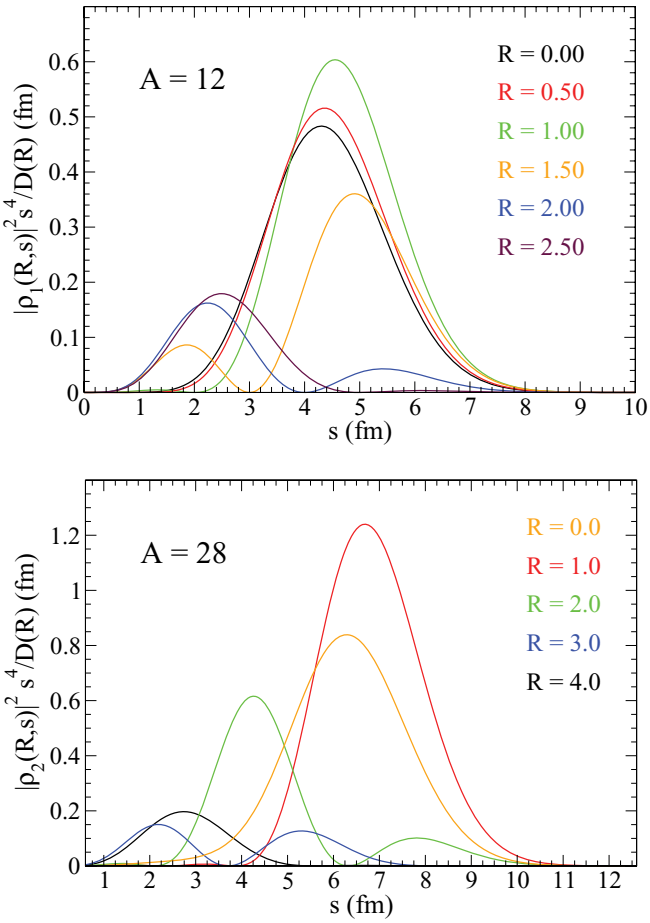

FIG. 4. (Color online) Normalized square of the density matrix $\rho(\mathbf{R}, \mathbf{s})$ multiplied by s^4 as a function of the relative coordinate s. In the top panel it is displayed for $A = 12$ ($N = 1$) and in the bottom panel for $A = 28$ ($N = 2$).

confinement. After the minimum, that is, more or less after the classical turning point (for very small systems the latter does not have such a well-defined meaning), the pair wave function enters the evanescent region and again slightly expands before reaching the asymptotic value. It also is worth mentioning that the minimum of the CL is very slowly increasing with particle number, approximately as $\sim A^{1/6}$. For $A = 8000$ the minimum value is about 4 fm. Once $\omega \to 0$, the CL approaches infinity everywhere. A generic feature also is that, independent of A, starting from the center at $R = 0$, the pairs first slightly expand up to $R \sim 1$ fm before becoming smaller getting closer to the border of the mean field. For these R values around the origin, the nodes lie in the region that is dominated by the phase space factors s^2 and s^4 in the integrals over s in Eq. (13) (i.e., well to the left of the maximum of the bump created by the function $s^4 e^{-\alpha^2 s^2/2}$). It can easily be verified from our "easy" example $N = 1$ [Eqs. (12) and (13)] that for very small values of R, the surface corresponding to the s integral of the denominator decreases faster than that of the numerator. Therefore, the CL increases. However, once the node comes into the region where the exponential regime takes over (i.e., where the extension of the system is felt), the CL starts its regression. These considerations may be elaborated in all details for the case $N = 1$ and also further be elucidated in considering as a complement to the density matrix $\rho_N(\mathbf{R}, \mathbf{s})$ its Wigner representation Eq. (2). Not to make the present discussion too heavy, we refrain from entering these more detailed considerations. The case $N = 1$ is, as seen, already characteristic and can be studied straightforwardly.

We also should mention that even in our averaging over major shells, orbit mixing *within* the shell takes place. The cross terms give rise to a destructive interference still lowering the minimum of the CL by a small but definite amount of about 0.5 fm from its nonaveraged values. This can be realized in comparing Fig. 6 where the CL, that is, local in R rms radii from individual HO orbits are displayed (for a precise definition, see [5]) with the dashed line in the top panel of Fig. 2.

Intrashell averaging, therefore, is present even in the limit of very small pairing with gap values of the order of subshell spacings. In Ref. [5] the same study is performed with the self-consistent HFB orbits (see Fig. 17 in that reference). It

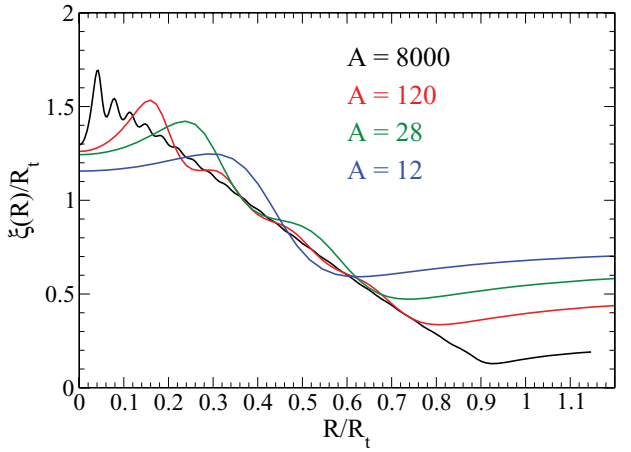

FIG. 5. (Color online) Coherence length (CL) for systems containing $A = 12, 28, 120$, and 8000 nucleons as a function of the radial distance R. Notice that both, coherence length and radial distance, have been scaled by the classical turning point distance R_t (see text).

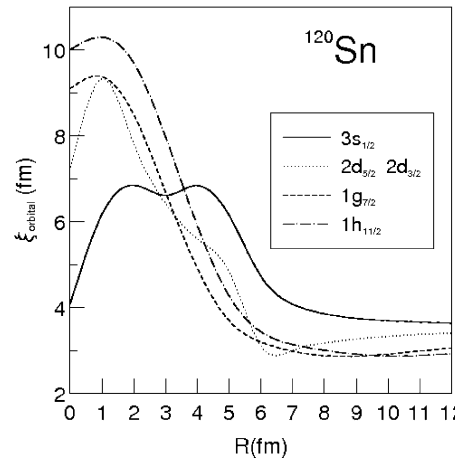

FIG. 6. Individual contributions to the CL in the HO model for $A = 120$ corresponding to the different individual orbitals of the last shell.

is seen that in the self-consistent case the reduction of the minimal value of the CL from intrashell mixing is about 30% and, therefore, somewhat stronger than in the present simplified HO model. Though not completely negligible, this interesting behavior is nonetheless a minor effect with respect to the feature we are discussing in this work, namely a surprising reduction of the minimal value of the CL by a factor 3–4 from a simple weak coupling estimate [7].

We, therefore, can say that in cases where, in finite Fermi systems, typical values of gap parameters around the Fermi energy are smaller than $\hbar\omega$ or energy differences between neighboring major shells in spherical nuclei, the size of Cooper pairs in superfluid nuclei, or other finite Fermi systems, is essentially determined by the spatial extension of the single-particle wave functions close to the Fermi energy. Passing for the sake of argument to a continuum version of Eq. (2) [i.e., $\kappa(\mathbf{R},\mathbf{p}) = \int dE \kappa(E) f_E(H_{\text{cl.}})$], we see that in nuclei where the width of $\kappa(E)$ is much smaller than the width of $f_E(H_{\text{cl.}})$, the CL is dominated by $f_E(H_{\text{cl.}})$ on the Fermi surface. Of course, a very different situation prevails in the opposite regime where $\Delta \gg \hbar\omega$. In the extreme case of infinite matter or $\hbar\omega \to 0$, we have $f_E(H_{\text{cl.}}) \to \delta(E - H_{\text{cl.}})$, and the ratio of the values of the widths is inversed! Simple scaling arguments show that in the latter case $\xi \sim 1/\Delta$, which also is reflected in the well-known expression given by Pippard [14],

$$\xi = \frac{1}{\pi}\frac{\hbar^2}{m}\frac{k_F}{\Delta}, \tag{22}$$

or by an equivalent formula given in the appendix of our preceding paper [5]. Therefore, in the infinite matter case the dependence on the gap is not at all compensated between numerator and denominator in Eq. (6), whereas this is the case in finite nuclei [see Eq. (9)].

As a consequence, the use of LDA, which is equivalent to the infinite matter regime, is not valid to estimate the coherence length in finite nuclei. For other quantities, however, as, for example, the pairing energy, LDA gives a reasonable good average [15]. Nevertheless, even in such favorable cases, LDA is very much at the limit of its validity, for instance, in what concerns a detailed description of the radius dependence of various pairing quantities. Further considerations on this subject will be published elsewhere [16].

In conclusion, concerning the extension of Cooper pairs in finite superfluid Fermi systems, we have identified two regimes: one for $\hbar\omega \gg \Delta$ where the coherence length is practically independent of Δ and determined by the spatial extension of the single-particle wave functions. In addition to nuclei, such a situation may be found in ultrasmall superconducting metallic grains [17,18]. In the second regime with $\hbar\omega \ll \Delta$, the coherence length is approximately inversely proportional to the gap values. The latter situation is, in addition to nuclear matter, for example, realized in cold superfluid fermionic atoms in traps where typical values of $\Delta/(\hbar\omega)$ may be of the order of 10 or even larger [19]. It would be interesting to study the crossover from one regime to the other in more detail.

Let us finally wrap up the situation of the CL in nuclei. We found that a simplest spherical HO model already simulates quite faithfully realistic HFB calculations with the Gogny force. In what concerns the CL, the situation for nuclei is such that there is very little difference between rms values of uncorrelated pairs coupled to $L = S = 0$ calculated locally as a function of the radius R and local Cooper pair sizes calculated with the nominal pairing interaction. Therefore, the small Cooper pair size of 2.0–2.5 fm in the surface of nuclei is practically entirely a finite size effect and has not much to do with existing enhancement of pairing in the nuclear surface. A very characteristic and generic pattern has emerged. In the lightest nuclei, like, for example, the α particle, their size is so small that the extension of a pair cannot reach more than 2 fm. Going to P shell nuclei, in the interior the pairs can already somewhat extend but approaching the border of the mean field they shrink until they again reach a value of around 2 fm from the restricted space around the surface. In the interior the pairs grow approximately with the size of the nucleus (see Fig. 5) but toward the surface they always regress to their very small value. In the evanescent region, the pair sizes become slightly larger than their minimum value in the surface region but this increase is very moderate. A characteristic feature also is that the pairs only feel the finite size from $R =$ 1 fm onward. Before, they slightly expand up to $R = 1$ fm, independent of the mass number of nuclei and of parity of the shell. This scenario of a first slight increase, followed by a longer linear descent, before going through a shallow minimum at 2.0–2.5 fm, leveling off in a slightly increased asymptotic value is practically a generic feature of local pair sizes in nuclei. It is seen in our schematic model, but also in realistic calculations (see Fig. 3 of [1]), though in the latter case some scatter exists, probably from more pronounced shell effects. This characteristic pattern of local Cooper pair sizes, practically independent of the strength of the pairing force as long as it stays below the nominal value, is one of the clearest theoretical manifestations that nuclei are in a weak coupling regime characterized by gap values $\Delta \ll \hbar\omega$. In the opposite limit $\Delta \gg \hbar\omega$, as prevails in infinite matter, but in the regime where $\Delta \ll \mu$ that is still in weak coupling [20], the coherence length varies inversely proportional to the gap, a fact that is well known. The fact that Cooper pair sizes are largely dominated by geometry should, however, not make us forget that for other quantities nuclear superfluidity has an enormous impact. To say it again, a particularly striking example, in addition to other more standard ones, is the effect of parity mixing on the spatial behavior of the nonlocal (unnormalized) pairing tensor, as revealed recently [3,5]. Indeed, this not normalized pairing tensor $\kappa(\vec{R},\vec{s})$ becomes very much localized in $\vec{s}$ around the $\vec{R}$ axis whereas the parity projected $\kappa(\vec{R},\vec{s})$ is completely delocalized [3,5] However, because of normalization in the coherence length this feature is canceled out.

ACKNOWLEDGMENTS

We appreciated very stimulating discussions with J.-F. Berger, A. Pastore, and N. Sandulescu. This work was partially supported by the IN2P3-MICINN agreement FPA2008-03865-E/IN2P3 and by the Spanish Consolider-Ingenio 2010 program CPAN CSD2007-00042. X.V. also acknowledges support from FIS2008-01661 (Spain and FEDER) and 2009SGR-1289 from Generalitat de Catalunya (Spain).

[1] N. Pillet, N. Sandulescu, and P. Schuck, Phys. Rev. C **76**, 024310 (2007).
[2] A. Pastore, F. Barranco, R. A. Broglia, and E. Vigezzi, Phys. Rev. C **78**, 024315 (2008).
[3] M. Matsuo, K. Mizuyama, and Y. Serizawa, Phys. Rev. C **71**, 064326 (2005).
[4] W. von Oertzen and A. Vitturi, Rep. Prog. Phys. **64**, 1247 (2001).
[5] N. Pillet, N. Sandulescu, P. Schuck, and J.-F. Berger, Phys. Rev. C **81**, 034307 (2010).
[6] J. Dechargé and D. Gogny, Phys. Rev. C **21**, 1568 (1980); J.-F. Berger, M. Girod, and D. Gogny, Comput. Phys. Commun. **63**, 365 (1991).
[7] A. Bohr and B. R. Mottelson, *Nuclear Structure* (Benjamin, Reading, MA, 1975), Chap. 6, p. 398.
[8] M. Prakash, S. Shlomo, and V. M. Kolomietz, Nucl. Phys. A **370**, 30 (1981).
[9] P. Ring and P. Schuck, *The Nuclear Many-Body Problem* (Springer-Verlag, New York, 1980).
[10] X. Viñas, P. Schuck, M. Farine, and M. Centelles, Phys. Rev. C **67**, 054307 (2003).
[11] G. G. Dussel, S. Pittel, J. Dukelsky, and P. Sarriguren, Phys. Rev. C **76**, 011302 (2007); G. Ortiz and J. Dukelsky, Phys. Rev. A **72**, 043611 (2005).
[12] S. S. Pankratov, E. E. Saperstein, M. V. Zverev, M. Baldo, and U. Lombardo, Phys. Rev. C **79**, 024309 (2009).
[13] As a matter of fact for values of $R < \frac{1}{2\alpha}$, no real nodes exist. This, however, does not perturb the general pattern of the bottom panel of Fig. 4 being qualitatively similar to that of the top panel.
[14] A. L. Fetter and J. D. Walecka, *Quantum Theory of Many-Particle Systems* (McGraw-Hill, New York, 1971).
[15] H. Kurchareck, P. Ring, P. Schuck, R. Bengston, and M. Girod, Phys. Lett. B **216**, 249 (1989).
[16] X. Viñas, M. Farine, and P. Schuck (in preparation).
[17] M. Farine, F. W. J. Hekking, P. Schuck, and X. Viñas, Phys. Rev. B **68**, 024507 (2003).
[18] J. von Delft and D. C. Ralph, Phys. Rep. **345**, 61 (2001).
[19] L. Pitaevskii and S. Stringari, *Bose-Einstein Condensation*, International Series of Monographs on Physics 116 (Oxford Science Publications, Clarendon Press, 2003).
[20] The criterion $\Delta/\mu \sim \Delta/\varepsilon_F \ll 1$ is, in the continuum limit, equivalent to the usual weak coupling estimate $G\rho$ (matrix element times level density at Fermi energy) $\ll 1$. However, in finite systems with shell structures, the additional distinction $\Delta/(\hbar\omega) \gtrless 1$ can be made influencing the details of pairing. A nice discussion of weak versus strong pairing in finite systems is given in Ref. [18].